Published in final edited form as:
Hepatology. 2012 January ; 55(1): 86–97. doi:10.1002/hep.24629.

Immunization with ASPH-loaded dendritic cells produces anti-tumor effects in a rat model of intrahepatic cholangiocarcinoma

Takehiro Noda[1], **Masafumi Shimoda**[1], **Vivian Ortiz**[1], **Alphonse E. Sirica**[2], and **Jack R. Wands**[1]

[1]The Liver Research Center, Department of Medicine, Rhode Island Hospital and Brown Medical School, Providence, Rhode Island, USA

[2]Department of Pathology, Division of Cellular and Molecular Pathogenesis, Virginia Commonwealth University School of Medicine, Richmond, VA

Abstract

Dendritic cells (DCs) capture, process proteins and present peptides on the cell surface in the context of major histocompatibility complex (MHC1 and MHC11) molecules to induce antigen-specific T cell immune responses. The aims of this study were to (1) employ an expanded and purified DCs population and load them with aspartate-β-hydroxylase (ASPH), a highly expressed tumor associated cell surface protein, and (2) to determine if immunization induced anti-tumor effects in an orthotopic rat model of intrahepatic cholangiocarcinoma (ICC). Splenocytes were incubated with ASPH-coated beads and passed through a magnetic field to yield an 80% pure DC OX62+ population. This DC subset was stimulated with GM-CSF, IL-4, CD40L and IFN-γ, resulting in a 40-fold increase in IL12A mRNA expression to subsequently generate a Th_1 type immune response. After incubation with the cytokine cocktail, DCs were found to have matured, as demonstrated by increased expression of CD40, CD80 and CD86 co-stimulatory molecules. Immunization with ASPH-loaded DCs induced antigen-specific immunity. A clone of the parental tumorigenic rat BDEneu cholangiocyte cell line, designated BDEneu-C24 found to have the highest number of cells expressing this surface protein (97%); it maintained the same phenotypic characteristics of the parental cell line and was used to produce intrahepatic tumors in immunocompetent syngeneic Fischer-344 rats. Immunization with ASPH-loaded DCs generated cytotoxicity against cholangiocarcinoma cells in vitro and significantly suppressed intrahepatic tumor growth and metastasis, and was associated with increased CD3+ lymphocyte infiltration into the tumors.

Conclusions—These findings suggest that immunization with ASPH-loaded DCs may constitute a novel therapeutic approach for ICC, since this protein also appears to be highly conserved and expressed on human hepatobiliary tumors.

Keywords

antigen presenting cells; bile duct tumors; immunotherapy; aspartyl-β-hydroxylase

Introduction

Cholangiocarcinoma is the second-most common primary liver tumor (10 to 15%) compared to hepatocellular carcinoma (HCC). The incidence and subsequent mortality of intrahepatic

Corresponding Author: Jack R. Wands, MD, The Liver Research Center, 55 Claverick Street, 4th Floor, Providence, Rhode Island, 02903, USA, Jack_Wands_MD@brown.edu Fax: +1-401- 444-2939.

Conflict of interest: The authors have declared that no conflict of interest exists.

cholangiocarcinoma (ICC) has been increasing worldwide (1). It is difficult to establish the diagnosis of early stage ICC, since symptoms are not prominent until the disease is far advanced. Patients with unresectable tumor have a dismal prognosis, with a median survival time of nine months (2, 3). Surgical resection is considered to be the most viable approach to attempt a "cure" for ICC; however, the five year survival rate ranges from 25% to 48% due to incomplete resection and subsequent high recurrence rate (~50%) (4–6). New approaches are urgently needed to prevent tumor recurrence after surgical resection in an attempt to further improve patient survival.

Aspartate-β-hydroxylase (ASPH), also known as aspartyl-asparaginyl β-hydroxylase, is a type 2 transmembrane protein belonging to the α-ketoglutarate-dependent dioxygenase family. This molecule catalyzes post-translational hydroxylation of beta carbons of aspartyl and asparaginyl residues in epidermal growth factor-like domains of certain proteins, including Notch and Notch homologs (7–12). Over-expression of ASPH produces a malignant phenotype characterized by increased cell motility and invasion (13). ASPH is abundantly expressed in a number of malignant neoplasms, which include HCC, ICC, lung, colorectal, pancreatic, and neural carcinomas (14–18). In contrast, most normal tissues have relatively low or absent ASPH expression (14), as measured by immunohistochemistry and "real time" RT-PCR. ASPH over-expression has been observed to contribute to the infiltrative growth pattern of cholangiocarcinoma cells by promoting cell motility (19). Moreover, surgically resected ICC tumors exhibited high level ASPH immunoreactivity in over 95% of cases, with the degree of ASPH overexpression appearing to correlate with tumor size, infiltrative growth pattern, histological grade, vascular invasion and poor survival rates (20).

DCs are professional antigen-presenting cells that capture and break-down proteins into immunogenic peptides that are subsequently presented with products of the major histocompatibility complex (MHC) to naïve T cells. Therefore, DCs induce a cellular immune response that involves both CD4+ T helper and cytolytic CD8+ T cells (21, 22). Due to their demonstrable antitumor effects, DCs have emerged as attractive candidates to deliver tumor associated antigens (TAAs) for tumor immunotherapy. In this study, our aim was to preclinically establish this approach as being potentially useful for the prevention and/or treatment of ICC by utilizing ASPH as a functional cell surface antigen delivered by DCs to an immunocompetent animal model of ICC closely resembling the progressive human disease.

Previously, we established a novel method of generating large numbers of DCs in mice by hydrodynamic delivery of plasmid DNA that encoded for the secreted form of human fms-like tyrosine kinase 3 ligand (hFlt3L) (23). DCs may be enriched from splenocytes *in vitro* by phagocytosis of magnetic beads and separation in a magnetic field. Here we demonstrate that a DC population was generated and characterized following hydrodynamic gene delivery of hFlt3L. In this context, immunotherapy using mature ASPH-loaded DCs was employed in an effort to induce antitumor effects against intrahepatic ICC tumors produced by injection of the highly tumorigenic rat BDEneu cholangiocyte cell line into the liver of syngeneic rats.

Methods

Cell lines and culture

BDEneu cells were cultured in Dulbecco's Modified Eagle Medium (DMEM) as previously described (24). Using the limiting dilution technique of BDEneu parental cell (BDEp), 10 clones of BDEneu cells were established. Among the 10 clones, BDEneu Clone 24 (BDE CL24) was used in the generation of ICC, since it had the highest percentage of cells

expressing ASPH on the cell surface. A murine hepatocellular carcinoma cell line, BNL 1ME A.7R.1 (BNL), obtained from American Type Culture Collection served as a positive control.

Animals, tumor challenge and immunization

Young adult Fischer 344 male rats (Harlan, Indianapolis, IN) with mean body weight of approximately 150 – 200 g were maintained in accordance with the guidelines set by the Institutional Animal Care and Use Committee of Rhode Island Hospital (Providence, RI) and used in the experiments described. The BDE CL24 cells were suspended in HBSS. A small incision was made and the bile duct was identified and ligated using non-absorbable silk surgical suture. BDE CL24 cells (3×10^6) were inoculated into the parenchyma of the left hepatic lobe through 30 gauge needle. After tumor cell inoculation at day 0, animals were immunized with 1×10^6 ASPH or GFP-loaded DCs 2 times at day 4 and day 8. Rats were euthanized at day 18 and tumor volumes were measured using a caliper, and volumes were calculated by the formula: V = length × width × height ×0.5. When the tumors were multiple, the largest three tumor volumes were calculated and the total tumor volume was determined.

In vivo generation of dendritic cells

The rat DC population was expanded by hydrodynamic delivery of plasmid DNA construct encoding the secreted form of hFlt3L (23) and the technique is described in detail under Supplemental Methods.

Flow cytometry analysis

The cell surface expression of ASPH in BDEneu and BDEneu C24 cells and other phenotypic markers expressed by purified DC populations were analyzed by flow cytometry as previously described (23). Details are supplied in Supplemental Methods.

Recombinant human aspartate-β-hydroxylase

The full length human ASPH (GenBank accession no. 583325) was cloned into the EcoRI site of the pcDNA vector (Invitrogen). Recombinant ASPH protein produced in a Baculovirus system (Invitrogen) according to manufacturer’s instruction.

Western blot analysis

Western blot analysis was done as previously described (25) and the antibodies used are described in the Supplemental Methods.

Cell proliferation and cytotoxicity assays

Descriptions are provided in Supplemental Methods.

Histochemical, immunohistochemical and immunofluorescent staining

Details are provided in the Supplemental Methods.

Quantitative reverse-transcription PCR analysis

Total RNA from cultured BDEneu cells, 5×10^6 freshly purified dendritic cells or stimulated dendritic cells was isolated and qPCR was performed as described (26). Primer sequences are provided in the Supplemental Methods.

Cytokine enzyme-linked immunosorbent assays and immunization with DCs

To examine the production of IL-10, 2×10^5 purified DCs per well were cultured in 96-well plates in RPMI 1640 medium in the presence of GM-CSF and/or IL-4 and/or IFN-γ and/or CD40L for 48 h. Culture supernatants were collected and subjected to enzyme-linked immunosorbent assay (ELISA) using OptEIA set ELISA kits (BD Biosciences) according to the manufacture's instructions. Immunization of rats with purified antigen-loaded DCs was performed as described (27). Details are provided in the Supplemental Methods.

Statistical analysis

Results were analyzed using the SPSS software (version 11.0.1 J, SPSS Inc., Chicago, IL). Data was analyzed by a non-paired Student's t-test or one-way analysis of variance followed by a Tukey test when comparing more than two groups. Differences are considered significant at $p<0.05$.

Results

Expansion and Purification of Dendritic Cells

The rat DC population was expanded and identified by the rat DC-specific integrin CD103 which is recognized by the OX62 antibody. The OX62+DCs can be further classified as two subsets based on the expression of the CD4 molecule i.e., CD4-OX62+DCs and CD4+OX62+DCs. The hFlt3L-treated splenocytes were comprised of approximately 30% of OX62+DC (28.4% of CD4-OX62+DCs and 3.8% of CD4+OX62+DCs) compared to just 1% of such a population residing in the normal spleen. Incubation of expanded splenocyte populations with magnetic beads followed by a purification step of the bead-containing cells via separation on a magnetic column, generated an enriched DC population consisting of greater than 80% OX62+DCs (73.8% of CD4-OX62+DCs and 6.6% of CD4+OX62+DCs) (Figure 1A). It is noteworthy that $5.0 – 7.0 \times 10^8$ splenocytes were obtained per hFlt3L-treated spleen. After purification of cells that phagocytized magnetic beads, the yield was found to be $4.0 – 6.0 \times 10^7$ DCs per spleen, and these cells had greater than 90% viability. The CD4-DC: CD4+DC ratio was approximately 1:1 in normal OX62+ cells compared with 7:1 in hFlt3L-treated OX62+ cells or 11:1 in OX62+ cells purified after phagocytosis of beads. Thus, the CD4-OX62+ subset was the major subpopulation found in purified DCs produced by this technique. Previously, rat plasmacytoid DCs (pDC) were identified as a subset of MHC class II+ CD4+CD3-CD11b-CD45R+ leukocytes and they have been found to produce large amounts of type I IFN upon viral stimulation. The pDC subset, as shown as the box in Figure 1B, was not able to be expanded by hydrodynamic injection of hFlt3L, nor further purified by phagocytosis of magnetic beads.

Phenotypic Characterization of the DC Population

The phenotype of DC subpopulations expanded by hFlt3L injection and purified by phagocytosis of magnetic beads was further analyzed after double staining using PE-conjugated anti-CD103 (OX62) or PE-conjugated anti-MHC class II (RT1B) and other FITC-conjugated antibodies (Figure 1C). The OX62+DCs showed negative expression of CD3, CD8a, CD45R and CD45RA. In addition, the OX62+DCs showed dull expression of CD161a (NKR-P1A) and positive expression of MHC class I, class II and CD11b. Previously, we have reported that a murine DC population expanded by hFlt3L injection and enriched by magnetic beads contained approximately 17% macrophages (23). The enriched rat DC population characterized here contained approximately 15% OX62-cells (Figure 1A) and half of the OX62- cells stained positive by anti-granulocyte antibody (HIS48). In contrast, the OX62- cells were negative for the macrophage markers CD68 (ED1), CD163 (ED2) and CD169 (ED3). But approximately 10% of these enriched DCs were positive for

another macrophage marker, HIS36, indicating the presence of macrophage subsets. The DCs isolated by positive selection using the OX62 antibody have been reported to be negative for co-stimulatory molecule (CD40 and CD86) expression (28). However, the DC population enriched by phagocytosis of magnetic beads shown here have a broad range of CD40 expression with no expression of CD86.

Differential IL12A and IL12B expression in activated DCs

We investigated the ability of DCs to produce IL-12 under stimulation with GM-CSF, IL-4, CD40L and IFN-γ. IL-12 is 70kD heterodimeric cytokine composed of two disulfide-linked subunits (p35 and p40) encoded by two separate genes. Bioactive IL-12p70 production by antigen-presenting DCs or macrophages is a key factor for initiation of CD4+ T helper 1 (Th_1) cell activation (29, 30). Furthermore, the IL-12p35 subunit plays a role as a limiting component which determines production of IL-12p70 since IL-12p35 is made at substantially lower levels than IL-12p40; therefore, IL-12p70 production is dependent on the level of IL-12p35 expression in the cell (31). The IL12A and IL12B mRNA expression levels produced by DCs in the culture medium or stimulated through GM-CSF, IL-4, CD40L or IFN-γ additions (24 h after purification with magnetic beads) were monitored. Both the IL12A and IL12B mRNA expression results were normalized to levels found in DCs before stimulation. The IL12A mRNA revealed highest expression (43.7 fold) 3 h after IL-4 stimulation (Figure 2A). In contrast, IL12B expression was optimal 6h after CD40L stimulation (16.0 fold) (Figure 2B). Next, studies were performed on IL12A expression by DCs stimulated with the cytokine cocktail (GM-CSF, IL-4, IFN-γ and CD40L) and measured 3h after stimulation. The cytokine cocktail induced IL12A mRNA expression approximately 40-fold compared with DCs cultured with medium alone (Figure 2C). Finally, the production of IL-10 was measured in culture supernatants 48 h after stimulation with cytokines either alone or in combination. The DCs stimulated by the full cytokine cocktail had a reduced IL-10 level compared to GM-CSF, IL-4 and CD40L stimulation (Figure 2D). From these results, we selected the combination of GM-CSF, IL-4, IFN-γ and CD40L as optimal activators of IL-12 production by DCs in further experiments.

Maturation of DCs by the Cytokines

Changes in co-stimulatory molecule expression on DCs after cytokine stimulation were evaluated. The DCs isolated by positive selection using an OX62 antibody exhibited lower expression of MHC class II and no expression of CD40, CD80 and CD86 co-stimulatory molecules and were considered as immature DCs. However, DCs freshly isolated following magnetic beads ingestion were found to have strong MHC class II expression and broad CD 40 expression. Thus, the final DC population purified by beads were considered to be of an intermediate maturity phenotype. The DCs stimulated by the cytokine cocktail for 40 h however, were considered mature because of the significantly higher expression levels of CD40, CD80 and CD86 co-stimulatory molecules (Figure 3).

Immunization with ASPH-loaded Dendritic Cells Induces Antigen-Specific Immunity

Splenocytes derived from rats immunized with ASPH-loaded DCs produced significantly higher amounts of IFN-γ, which increased substantially when cells were incubated with increasing concentrations of recombinant ASPH protein added to the culture medium (Figure 4A). Increased production of IFN-γ was not observed in splenocytes derived from controls subcutaneously immunized with HBSS or GFP-loaded DCs. In contrast, splenocytes derived from controls and animals inoculated with ASPH or GFP-loaded DCs were similar with respect to their capability to produce low level IL-4 and these low levels were not influenced by the presence of various concentrations of recombinant ASPH protein in the culture medium (Figure 4B).

Establishment and Characterization of BDEneu Subclones with High Expression of ASPH

The BDEneu parental (BDEneu-p) cell line was derived from rat cholangiocytes (BDE1) stably transfected to express a mutationally activated rat *neu* oncogene (32). In addition, BDEneu have been shown to be a transplantable cell line, and an animal model of ICC has been developed (24) to explore the anti-tumor effects of ASPH-loaded DCs. In this context, the cell surface expression of ASPH by the BDEneu cell line was analyzed by flow cytometry. The highly positive murine HCC cell line (BNL) was used as a positive control. BDEneu-p cells showed ASPH expression on approximately 85% of the cells, and there was a dimorphic population visible by light microscopy indicating a mixture of cell types. Using the limited dilution technique of BDEneu cells, 10 subclones were established and analyzed. Among these subclones, the BDEneu-CL24 cell line exhibited the highest percent of positive cells (97%) which expressed ASPH and it remained constant over 15 serial passages; this clone was selected for the immunotherapy experiments (Figure 5A). The BDE CL24 clone was further characterized and comparisons were made to BDEneu- p cells (Figure 5B).

The BDEneu-p and BDEneu-CL24 cell lines revealed comparable expression and phosphorylation of HER2/neu. The BDEneu-CL24 cells showed comparable levels of Akt and p-Akt expression; there was a slight reduction of p44/42 MAPK phosphorylation in BDEneu-CL24 compared with BDEneu-p cells. The expression levels of Cytokeratin 19, ASPH and Jagged1 in BDEneu-p and BDEneu-CL24 cells were similar. In contrast, Notch 1 protein expression was increased in BDEneu-CL24. The mucin 1 mRNA expression levels in both BDEneu-p and BDEneu-CL24 cells were analyzed by quantitative RT-PCR and showed no significant difference (Fig. 5C). The BDEneu-CL24 clone had similar cell proliferation potential compared to BDEneu-p cells (Fig. 5D). The BDEneu-CL24 cells produced ductal carcinomas at a 100% incidence after bile duct ligation and direct implantation into the left lobe of the liver which was identical to the BDEneu-p cell line. Histopathological evaluation of the intrahepatic tumors formed from the BDEneu-p and BDEneu-CL24 cells revealed ductal and trabecular growth patterns of tumor cells growth; both developed multiple areas of intrahepatic metastasis. In addition, there was an extensive intrahepatic irregular collagen deposition pattern representative of dense stroma formation in reaction to tumor cell growth. Tumors derived from both cell lines demonstrated positive immunoreactivity for HER2/neu and ASPH protein expression (Figure 6); normal rat heart, lung, liver, kidney and brain were negative for ASPH expression (data not shown).

Immunization with ASPH-loaded DCs Induced Cytotoxicity and Inhibited ICC Growth

In vitro experiments were performed to determine if splenocytes derived from rats immunized with ASPH-loaded DCs induced cytotoxicity against BDEneu-CL24 rat cholangiocarcinoma target cells as shown in Figure 7A; such lymphocytes exhibited striking cell killing at various lymphocyte/target cell ratios.

More important, were the observations in vivo; animals were immunized with ASPH or GFP-loaded DCs two times on day 4 and day 8 after bile duct ligation and tumor cell implantation into the left lobe of the liver. As shown in Figure 7B, control rats treated with GFP-loaded DCs showed rapid ICC tumor growth (white arrow) with extensive intrahepatic spread (arrow heads). In contrast, immunization with ASPH-loaded DCs significantly suppressed tumor growth and intrahepatic spread compared with the non-relavent antigenic control. The mean tumor volume was significantly less in animals treated with ASPH-loaded DCs compared to those treated with GFP-loaded DCs ($p<0.05$) (Figure 7B). It was of interest that the residual tumors derived from the ASPH-DC immunized rats still expressed ASPH on the cholangiocarcinoma tumor cell surface indicating that “escape mutants” had not developed. Thus, more than two immunizations may be necessary to achieve optimal

anti-tumor effects in future studies. In addition, the effect of ASPH-loaded DCs immunization therapy on lymphocyte infiltration into tumors was investigated. We found that immunotherapy with ASPH-loaded DCs resulted in increased T cell infiltration (CD3+ cells) into tumors by immunohistochemical analysis (Figure 7C).

Discussion

This study demonstrates that immunotherapy with the ASPH-loaded DCs generated anti-tumor effects against ICC in an animal model system. Animal models of ICC have been difficult to develop. Sirica *et al.* (24) has successfully established and characterized a novel tumorgenic cholangiocyte derived cell line, BDEneu, which produced ICC in the Fischer 344 rat strain. Importantly, the identification of cell surface markers has facilitated the isolation and characterization of rat DC populations from the spleen to make immunotherapy feasible as shown here. The establishment of DC-based immunotherapy in a suitable ICC animal model provides opportunities to evaluate new anti-tumor approaches.

DCs are professional antigen-presenting cells that show an extraordinary ability to stimulate naïve T cells and to initiate primary adaptive immune responses. Because of this property, DCs are excellent candidates as vehicles for therapeutic and prophylactic immunizations against neoplasms. ASPH appeared to have attractive properties since it was a transmembrane cell surface protein highly conserved and expressed on most tumor cells in human cholangiocarcinomas, and not on surrounding proliferating normal bile ducts and liver parenchyma (13, 14, 19, 20). Furthermore, expression levels correlated with tumor recurrence and patient survival following surgical resection (20). The protein has well-defined biologic functions by promoting the transformed phenotype through promotion of increased cell migration, invasion, and proliferation (19). ASPH biologic activity involves an interaction with the Notch signaling cascade known to be important in cell migration (33). To deliver ASPH as an immunogen, we characterized a rat DC population following hydrodynamic gene delivery of hFlt3L expression plasmid. After maturation with cytokines, purified antigen-loaded DCs were injected subcutaneously to induce an antigen-specific host immune responses in the rat model of ICC. This investigation suggests that immunization of rats with ASPH-loaded DCs may induce substantial antitumor effects against orthotropic intrahepatic cholangiocarcinomas produced by hepatic injection of BDE CL 24 cells.

To achieve anti-tumor activity, it was necessary to generate and purify sufficient numbers of DCs with high viability. The selection approach to purify DCs from normal rat spleen was a major method used to accumulate sufficient cells with the desired phenotype for immunization studies as previously described (23). The yield was found to be $3–5 \times 10^6$ OX62+ cells per normal rat spleen (28). In contrast, *in vivo* DC expansion by hydrodynamic gene delivery of a hFlt3L expression plasmid yields $4.0 – 6.0 \times 10^7$ DCs which is 10 times more than the amount of DCs isolated without such stimulation.

DCs are divided into different subsets and those derived from the rat spleen express the DC-specific integrin CD103 recognized by the OX62 mAb (34). The OX62+ DCs are further divided into two subsets based on CD4+ and CD4- expression. The CD4- DC subset is the main producer of IL-12 and induced the Th_1 immune responses, whereas CD4+ DC do not produce bioactive IL-12 (28). The rat pDCs do not express the DC-specific OX62 marker and are generally defined by expression of MHC class II, CD3, CD4, CD45R and CD11b antigens. Rat pDCs produce type I interferon upon stimulation with oligonucleotides containing type B CpG motifs (35). Voisine et al demonstrated that the CD4- DCs produced robust amounts of the IL-12 proinflammatory cytokines and induced Th_1 responses whereas CD4+ DCs were found to have low levels of IL-12 expression. The DC population which exhibits the highest expression level of IL12A mRNA after stimulation with the four GM-

CSF, IL-4, IFN-γ and CD40L cytokines, will subquently augment optimal Th_1 and CTL responses. More important, IL-10 production by rat DCs was limited and would provide less suppression of beneficial Th_1 type anti-tumor immune responses.

The maturation status of DCs is critical for activating the appropriate effector T cells. Immature DCs function as antigen-capturing cells, whereas mature DCs represent potent antigen-presenting cells. The maturation of DCs is associated with the expression of co-stimulatory molecules such as CD40, CD80 and CD86 (36, 37). In this study, the freshly purified DCs generated after phagocytosis of magnetic beads from a mixed splenocyte population were negative for CD80 and CD86 antigens but demonstrated broad expression of CD40. Our laboratory previously demonstrated that the DCs incubated with un-coated (antigen negative) beads exhibit very low expression of CD40 in mice (23). This finding suggests that during the process of purification by magnetic beads, an intermediate maturation status of DCs occurs in the rat. Culture of rat DCs without any cytokine addition leads to spontaneous maturation and such cells are moderately positive for CD40, CD80 and CD86 expression; however, the addition of four cytokines to the culture medium results in a striking increase of CD80 and CD86 expression. This finding is consistent with previous observation suggesting that CD40L or GM-CSF triggers strong CD80 and CD86 expression on CD4- DCs (28, 38, 39).

In this context, immunization with ASPH-loaded DCs produced striking cytotoxicity against cholangiocarcinoma cells in vitro as shown in Figure 7A. To investigate the mechanism(s) of anti-tumor effects, we examined the tumor-infiltrating lymphocyte population in the tumors treated with GFP-loaded (control) or ASPH-loaded DCs. We found increased tumor-infiltrating CD3+ lymphocytes which suggest that the ASPH-loaded DC immunization approach may foster anti-tumor activity via recruiting T cells into the tumor. It is important to note that BDEneu-p and the clonal BDEneu-CL24 cells elicit a dense collagenous stromal response during tumor formation; yet CD3+ T cells were able to penetrate this barrier and reduce or retard established ICC tumor growth. We also examined ASPH expression of the residual tumor after immunization x2 with ASPH-loaded DCs. The remaining tumor cells still express ASPH on the cell surface. These findings suggest that additional immunizations may be required to achieve optimal anti-tumor activity and that “escape” tumors did not develop under these conditions. Finally, this general approach may be attractive for other human malignancies since hepatocellular, pancreas, colon and breast carcinomas have also been found to highly express ASPH on the tumor cell surface (14).

Supplementary Material

Refer to Web version on PubMed Central for supplementary material.

Abbreviations

ICC	intrahepatic cholangiocarcinoma
ASPH	aspartate-beta-hydroxylase
DC	dendritic cell
MHC	major histocompatibility complex
hFlt3L	human fms-like tyrosine kinase 3 ligand
PCR	polymerase chain reaction
RT	reverse-transcription

ELISA	enzyme-linked immunosorbent assay
pDC	plasmacytoid dendritic cell
PE	phycoerythrin
FITC	fluorescein isothiocyanate
GFP	green fluorescent protein

Acknowledgments

This work was supported by CA-123544 (J.R.W) and CA-83650 (A.E.S) from the National Institutes of Health and a grant from the Uehara Memorial Foundation, Japan.

References

1. Shaib YH, Davila JA, McGlynn K, El-Serag HB. Rising incidence of intrahepatic cholangiocarcinoma in the United States: a true increase? J Hepatol. 2004; 40:472–477. [PubMed: 15123362]
2. Weber SM, Jarnagin WR, Klimstra D, DeMatteo RP, Fong Y, Blumgart LH. Intrahepatic cholangiocarcinoma: resectability, recurrence pattern, and outcomes. J Am Coll Surg. 2001; 193:384–391. [PubMed: 11584966]
3. Endo I, Gonen M, Yopp AC, Dalal KM, Zhou Q, Klimstra D, D'Angelica M, et al. Intrahepatic cholangiocarcinoma: rising frequency, improved survival, and determinants of outcome after resection. Ann Surg. 2008; 248:84–96. [PubMed: 18580211]
4. Konstadoulakis MM, Roayaie S, Gomatos IP, Labow D, Fiel MI, Miller CM, Schwartz ME. Fifteen-year, single-center experience with the surgical management of intrahepatic cholangiocarcinoma: operative results and long-term outcome. Surgery. 2008; 143:366–374. [PubMed: 18291258]
5. Ercolani G, Vetrone G, Grazi GL, Aramaki O, Cescon M, Ravaioli M, Serra C, et al. Intrahepatic cholangiocarcinoma: primary liver resection and aggressive multimodal treatment of recurrence significantly prolong survival. Ann Surg. 252:107–114. [PubMed: 20531002]
6. DeOliveira ML, Cunningham SC, Cameron JL, Kamangar F, Winter JM, Lillemoe KD, Choti MA, et al. Cholangiocarcinoma: thirty-one-year experience with 564 patients at a single institution. Ann Surg. 2007; 245:755–762. [PubMed: 17457168]
7. Korioth F, Gieffers C, Frey J. Cloning and characterization of the human gene encoding aspartyl beta-hydroxylase. Gene. 1994; 150:395–399. [PubMed: 7821814]
8. Gronke RS, VanDusen WJ, Garsky VM, Jacobs JW, Sardana MK, Stern AM, Friedman PA. Aspartyl beta-hydroxylase: in vitro hydroxylation of a synthetic peptide based on the structure of the first growth factor-like domain of human factor IX. Proc Natl Acad Sci U S A. 1989; 86:3609–3613. [PubMed: 2726737]
9. Gronke RS, Welsch DJ, VanDusen WJ, Garsky VM, Sardana MK, Stern AM, Friedman PA. Partial purification and characterization of bovine liver aspartyl beta-hydroxylase. J Biol Chem. 1990; 265:8558–8565. [PubMed: 2187868]
10. Jia S, VanDusen WJ, Diehl RE, Kohl NE, Dixon RA, Elliston KO, Stern AM, et al. cDNA cloning and expression of bovine aspartyl (asparaginyl) beta-hydroxylase. J Biol Chem. 1992; 267:14322–14327. [PubMed: 1378441]
11. Jia S, McGinnis K, VanDusen WJ, Burke CJ, Kuo A, Griffin PR, Sardana MK, et al. A fully active catalytic domain of bovine aspartyl (asparaginyl) beta-hydroxylase expressed in Escherichia coli: characterization and evidence for the identification of an active-site region in vertebrate alpha-ketoglutarate-dependent dioxygenases. Proc Natl Acad Sci U S A. 1994; 91:7227–7231. [PubMed: 8041771]
12. Dinchuk JE, Focht RJ, Kelley JA, Henderson NL, Zolotarjova NI, Wynn R, Neff NT, et al. Absence of post-translational aspartyl beta-hydroxylation of epidermal growth factor domains in

mice leads to developmental defects and an increased incidence of intestinal neoplasia. J Biol Chem. 2002; 277:12970–12977. [PubMed: 11773073]

13. Ince N, de la Monte SM, Wands JR. Overexpression of human aspartyl (asparaginyl) beta-hydroxylase is associated with malignant transformation. Cancer Res. 2000; 60:1261–1266. [PubMed: 10728685]
14. Lavaissiere L, Jia S, Nishiyama M, de la Monte S, Stern AM, Wands JR, Friedman PA. Overexpression of human aspartyl(asparaginyl)beta-hydroxylase in hepatocellular carcinoma and cholangiocarcinoma. J Clin Invest. 1996; 98:1313–1323. [PubMed: 8823296]
15. Sepe PS, Lahousse SA, Gemelli B, Chang H, Maeda T, Wands JR, de la Monte SM. Role of the aspartyl-asparaginyl-beta-hydroxylase gene in neuroblastoma cell motility. Lab Invest. 2002; 82:881–891. [PubMed: 12118090]
16. Wang J, de la Monte SM, Sabo E, Kethu S, Tavares R, Branda M, Simao L, et al. Prognostic value of humbug gene overexpression in stage II colon cancer. Hum Pathol. 2007; 38:17–25. [PubMed: 17020779]
17. Luu M, Sabo E, de la Monte SM, Greaves W, Wang J, Tavares R, Simao L, et al. Prognostic value of aspartyl (asparaginyl)-beta-hydroxylase/humbug expression in non-small cell lung carcinoma. Hum Pathol. 2009; 40:639–644. [PubMed: 19200576]
18. Palumbo KS, Wands JR, Safran H, King T, Carlson RI, de la Monte SM. Human aspartyl (asparaginyl) beta-hydroxylase monoclonal antibodies: potential biomarkers for pancreatic carcinoma. Pancreas. 2002; 25:39–44. [PubMed: 12131769]
19. Maeda T, Sepe P, Lahousse S, Tamaki S, Enjoji M, Wands JR, de la Monte SM. Antisense oligodeoxynucleotides directed against aspartyl (asparaginyl) beta-hydroxylase suppress migration of cholangiocarcinoma cells. J Hepatol. 2003; 38:615–622. [PubMed: 12713872]
20. Maeda T, Taguchi K, Aishima S, Shimada M, Hintz D, Larusso N, Gores G, et al. Clinicopathological correlates of aspartyl (asparaginyl) beta-hydroxylase over-expression in cholangiocarcinoma. Cancer Detect Prev. 2004; 28:313–318. [PubMed: 15542253]
21. Banchereau J, Steinman RM. Dendritic cells and the control of immunity. Nature. 1998; 392:245–252. [PubMed: 9521319]
22. Banchereau J, Palucka AK. Dendritic cells as therapeutic vaccines against cancer. Nat Rev Immunol. 2005; 5:296–306. [PubMed: 15803149]
23. Gehring S, Gregory SH, Wintermeyer P, San Martin M, Aloman C, Wands JR. Generation and characterization of an immunogenic dendritic cell population. J Immunol Methods. 2008; 332:18–30. [PubMed: 18258252]
24. Sirica AE, Zhang Z, Lai GH, Asano T, Shen XN, Ward DJ, Mahatme A, et al. A novel "patient-like" model of cholangiocarcinoma progression based on bile duct inoculation of tumorigenic rat cholangiocyte cell lines. Hepatology. 2008; 47:1178–1190. [PubMed: 18081149]
25. Toyama T, Lee HC, Koga H, Wands JR, Kim M. Noncanonical Wnt11 inhibits hepatocellular carcinoma cell proliferation and migration. Mol Cancer Res. 8:254–265. [PubMed: 20103596]
26. Merle P, Kim M, Herrmann M, Gupte A, Lefrancois L, Califano S, Trepo C, et al. Oncogenic role of the frizzled-7/beta-catenin pathway in hepatocellular carcinoma. J Hepatol. 2005; 43:854–862. [PubMed: 16098625]
27. Kuzushita N, Gregory SH, Monti NA, Carlson R, Gehring S, Wands JR. Vaccination with protein-transduced dendritic cells elicits a sustained response to hepatitis C viral antigens. Gastroenterology. 2006; 130:453–464. [PubMed: 16472599]
28. Voisine C, Hubert FX, Trinite B, Heslan M, Josien R. Two phenotypically distinct subsets of spleen dendritic cells in rats exhibit different cytokine production and T cell stimulatory activity. J Immunol. 2002; 169:2284–2291. [PubMed: 12193693]
29. Hsieh CS, Macatonia SE, Tripp CS, Wolf SF, O'Garra A, Murphy KM. Development of TH1 CD4+ T cells through IL-12 produced by Listeria-induced macrophages. Science. 1993; 260:547–549. [PubMed: 8097338]
30. O'Garra A. Cytokines induce the development of functionally heterogeneous T helper cell subsets. Immunity. 1998; 8:275–283. [PubMed: 9529145]
31. Snijders A, Hilkens CM, van der Pouw Kraan TC, Engel M, Aarden LA, Kapsenberg ML. Regulation of bioactive IL-12 production in lipopolysaccharide-stimulated human monocytes is

determined by the expression of the p35 subunit. J Immunol. 1996; 156:1207–1212. [PubMed: 8557999]

32. Lai GH, Zhang Z, Shen XN, Ward DJ, Dewitt JL, Holt SE, Rozich RA, et al. erbB-2/neu transformed rat cholangiocytes recapitulate key cellular and molecular features of human bile duct cancer. Gastroenterology. 2005; 129:2047–2057. [PubMed: 16344070]
33. Cantarini MC, de la Monte SM, Pang M, Tong M, D'Errico A, Trevisani F, Wands JR. Aspartyl-asparagyl beta hydroxylase over-expression in human hepatoma is linked to activation of insulin-like growth factor and notch signaling mechanisms. Hepatology. 2006; 44:446–457. [PubMed: 16871543]
34. Brenan M, Puklavec M. The MRC OX-62 antigen: a useful marker in the purification of rat veiled cells with the biochemical properties of an integrin. J Exp Med. 1992; 175:1457–1465. [PubMed: 1588275]
35. Hubert FX, Voisine C, Louvet C, Heslan M, Josien R. Rat plasmacytoid dendritic cells are an abundant subset of MHC class II+ CD4+CD11b-OX62- and type I IFN-producing cells that exhibit selective expression of Toll-like receptors 7 and 9 and strong responsiveness to CpG. J Immunol. 2004; 172:7485–7494. [PubMed: 15187127]
36. Larsen CP, Ritchie SC, Pearson TC, Linsley PS, Lowry RP. Functional expression of the costimulatory molecule, B7/BB1, on murine dendritic cell populations. J Exp Med. 1992; 176:1215–1220. [PubMed: 1328465]
37. Inaba K, Witmer-Pack M, Inaba M, Hathcock KS, Sakuta H, Azuma M, Yagita H, et al. The tissue distribution of the B7-2 costimulator in mice: abundant expression on dendritic cells in situ and during maturation in vitro. J Exp Med. 1994; 180:1849–1860. [PubMed: 7525841]
38. Grauer O, Wohlleben G, Seubert S, Weishaupt A, Kampgen E, Gold R. Analysis of maturation states of rat bone marrow-derived dendritic cells using an improved culture technique. Histochem Cell Biol. 2002; 117:351–362. [PubMed: 11976908]
39. Trinite B, Chauvin C, Peche H, Voisine C, Heslan M, Josien R. Immature CD4- CD103+ rat dendritic cells induce rapid caspase-independent apoptosis-like cell death in various tumor and nontumor cells and phagocytose their victims. J Immunol. 2005; 175:2408–2417. [PubMed: 16081812]

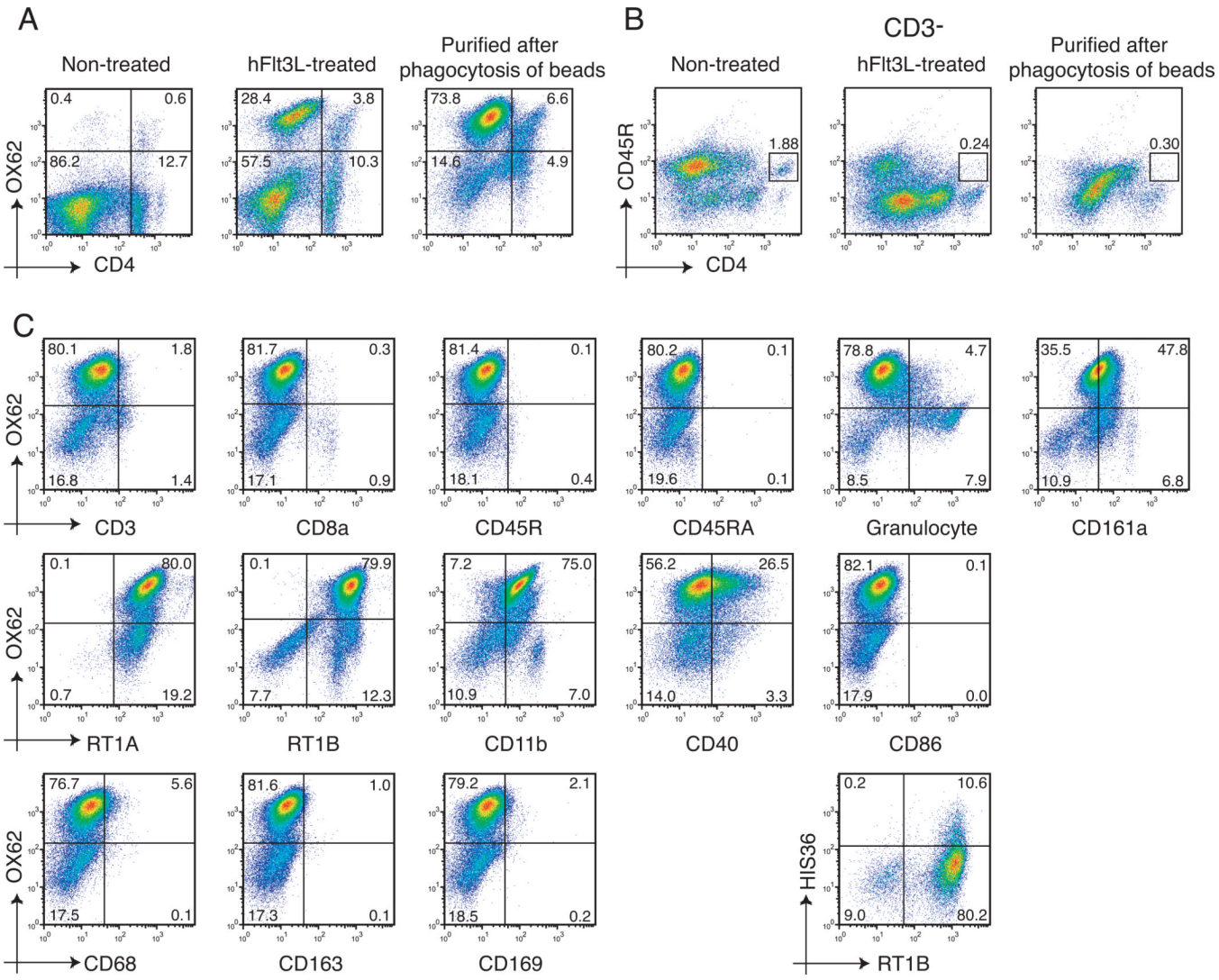

Figure 1. Flow cytometry analysis of cell surface markers on purified DCs

(**A**) The changes observed in the OX62+DCs population obtained from non-expanded (normal) expanded and purified from splenocyte populations. Cells are displayed in a OX62 and CD4 plot. (**B**) Detection of pDCs (CD3-CD4+CD45R+) in non-treated (normal), hFlt3L-treated splenocytes, or purified after phagocytosis of beads using flow cytometry. (**C**) The phenotype of the hFlt3L stimulated and purified DC population. To detect the HIS36+ cells, cells were stained with PE-conjugated anti-macrophage subset (HIS36) antibody and FITC-conjugated anti-RT1B antibody.

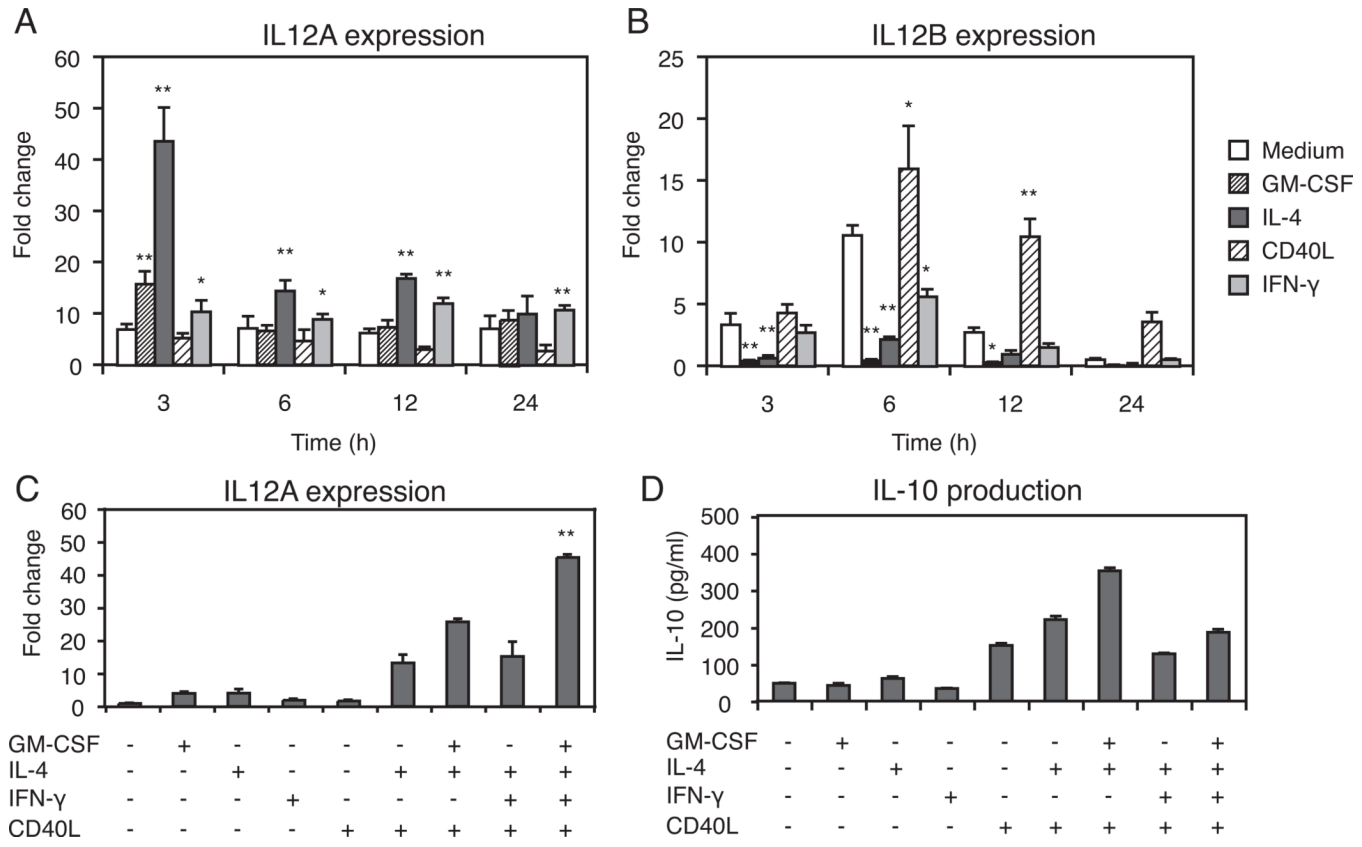

Figure 2. Cytokine expression in purified DCs

(**A**) Transient expression of IL12A mRNA of the IL-12p35 subunit in purified DCs stimulated for the indicated times with GM-CSF (4 ng/ml), IL-4 (100 ng/ml), or CD40L (1 μg/ml), or IFN-γ (20 ng/ml). (**B**) The expression of IL12B mRNA of the IL-12p40 subunit after cytokine stimulation. In panel (**A**) and (**B**), the expression of IL12A mRNA or IL12B mRNA was normalized to ribosomal 18S as measured in parallel reactions. The fold change was shown as the ratio to the expression level of IL12A mRNA or IL12B mRNA derived from DCs at 0 h without cytokine stimulation. *, $p<0.05$; **, $p<0.01$, as compared with cells cultured in medium alone. (**C**) Effects of the cytokine cocktail of GM-CSF, IL-4, IFN-γ, and CD40L either alone or in combination on the expression of IL12A mRNAs. The fold change is shown as the ratio to the expression level of IL12A mRNA from DCs at 3h without cytokine additions. **Significantly higher than the other groups ($p<0.01$). (**D**) IL-10 production by purified DCs cultured with cytokines either alone or in combination for 48 hours. Each value in all panels represents the mean ± SD.

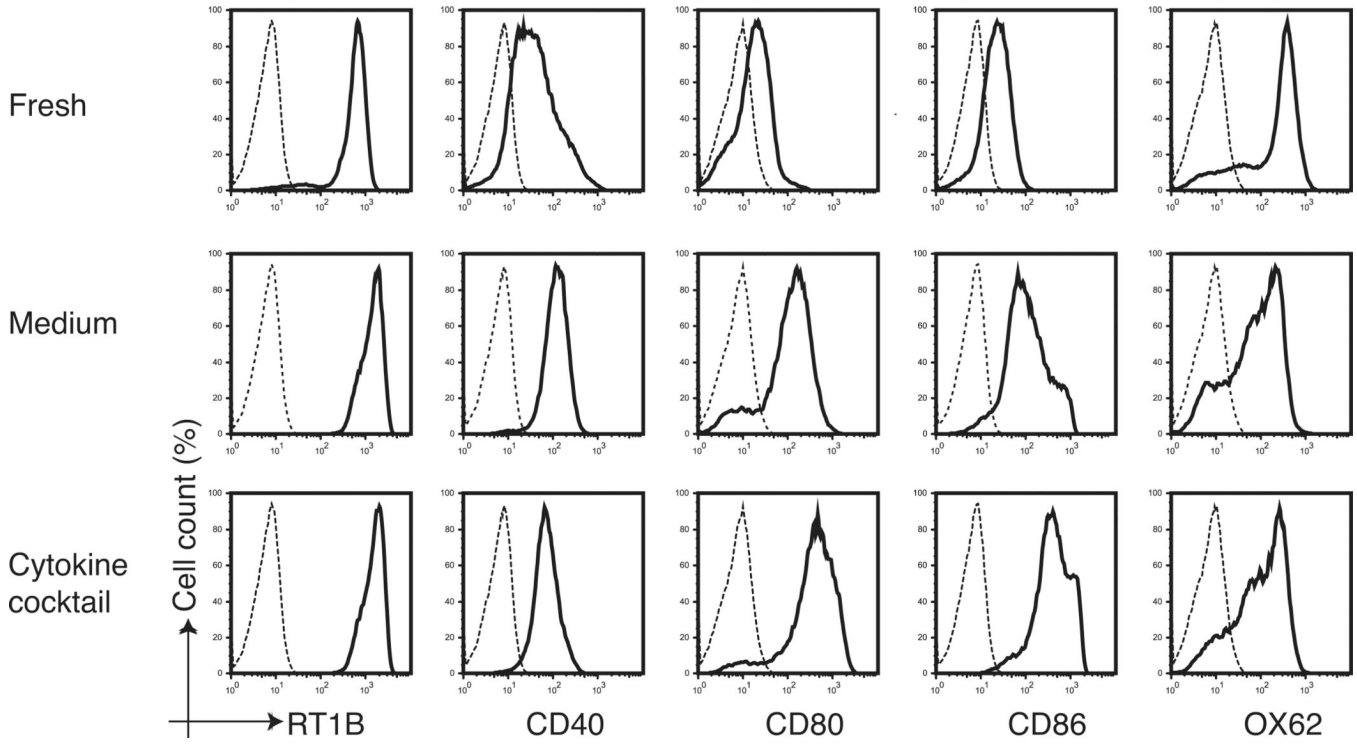

Figure 3. In vitro maturation of DCs following stimulation with the cytokine cocktail

The cytokine cocktail induced phenotypic maturation of purified DCs. The expression of RT1B, CD40, CD80, CD86 and OX62 (solid lines) were assessed by flow cytometry on freshly purified DCs or the same cells cultured for 40 hours in the presence or absence (medium) of GM-CSF (4 ng/ml), IL-4 (100 ng/ml), IFN-γ (20 ng/ml), and CD40L (1 μg/ml) added to the culture medium. The dashed line represents isotype-matched control antibodies.

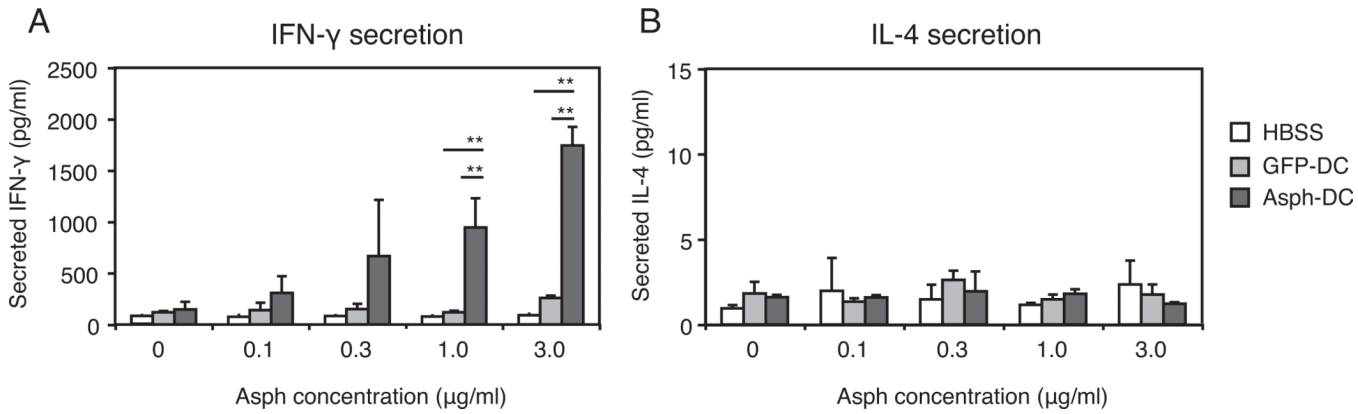

Figure 4. Antigen-specific responses of splenocytes derived from rat immunized with ASPH-loaded DCs

(**A**) Rats were subcutaneously immunized 2X at 2-week intervals with HBSS or with media that contained 1×10^6 ASPH-or GFP-loaded DCs. Splenocytes were harvested at 2 weeks after the second immunization and cultured for 48 hours in the presence of recombinant ASPH at the concentration indicated. Immunization with DCs purified via ingestion of ASPH-loaded beads exhibited antigen-specific IFN-γ secretion. (**B**) IL-4 secretion levels were similar in splenocytes derived from rats immunized with HBSS, GFP or ASPH-loaded DCs. Each value in all panels represents the mean ± SD. **, $p<0.01$.

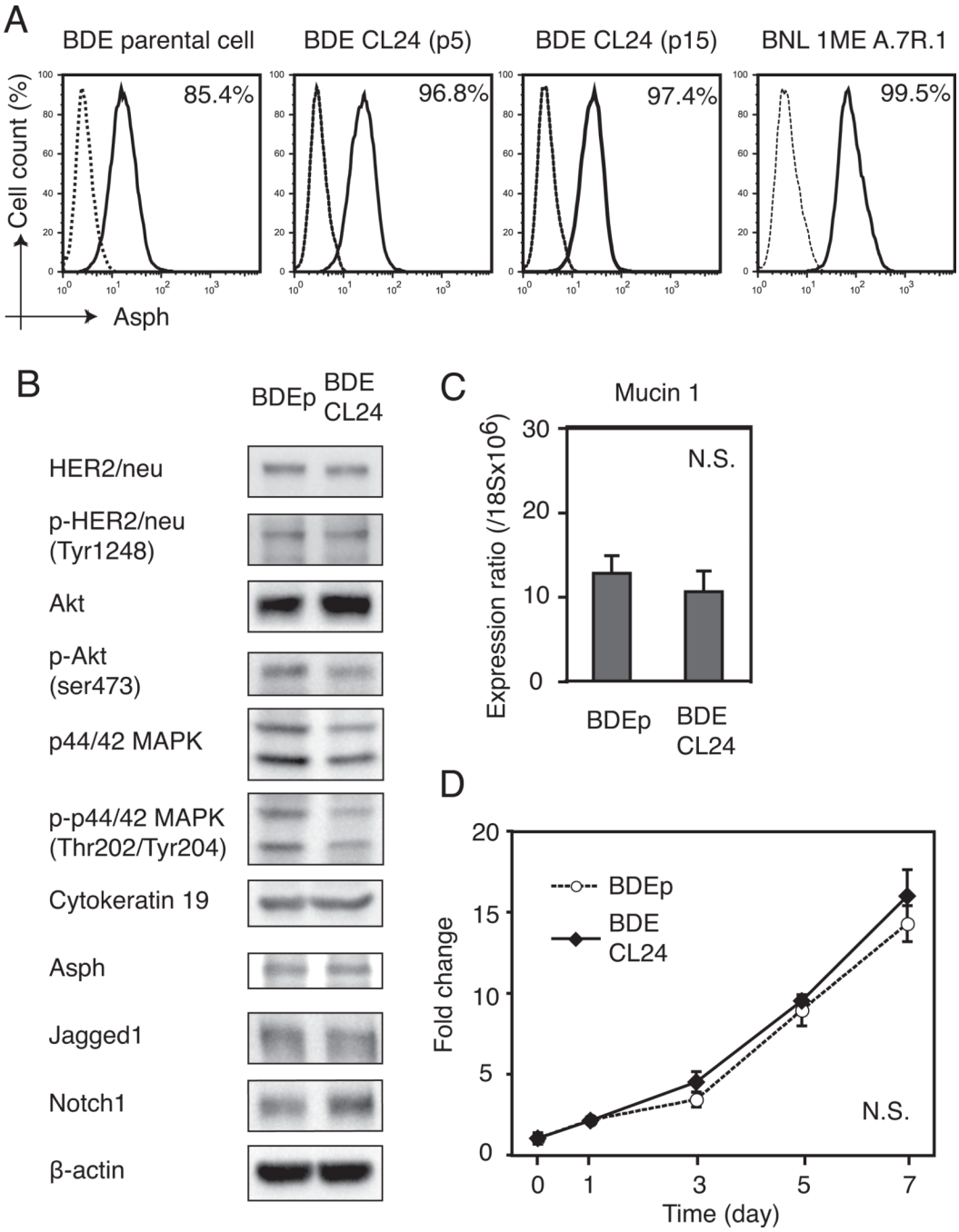

Figure 5. Establishment and characterization of BDEneu-CL24 cells with a high percent of cells that express ASPH on the plasma membrane

(**A**) Cell surface ASPH expression in BDEneu-p, BDE CLneu-CL24 at passage 5 and 15 respectively (BDEneu-CL24 p5 and BDEneu-CL24 p15) along with the murine BNL HCC cell line (positive control) using flow cytometery analysis. The percent of ASPH positive cells was determined by comparison with the isotype-matched control antibody (dashed line). (**B**) The BDEneu-CL24 cell showed similar protein expression patterns to BDEneu-p cells in signaling pathways related to HER2/neu by Western blot analysis. In contrast, the BDEneu-CL24 cell revealed increased Akt expression with reduced Akt and p44/42 MAPK phosphorylation levels. Notch 1 expression was also up-regulated in the BDEneu-CL24 cell

line. (**C**) The BDEneu- CL24 cells maintained high mucin 1 mRNA expression levels similar to the parental cell line (BDEneu-p); mucin 1 mRNA expression was normalized to ribosomal 18S. (**D**) Cell proliferation kinetics of BDEneu-p and BDEneu-CL24 cells were similar. Results were normalized by the average absorbance measured at day 0. Each value in panels (**C**) and (**D**) represents the mean ± SD.

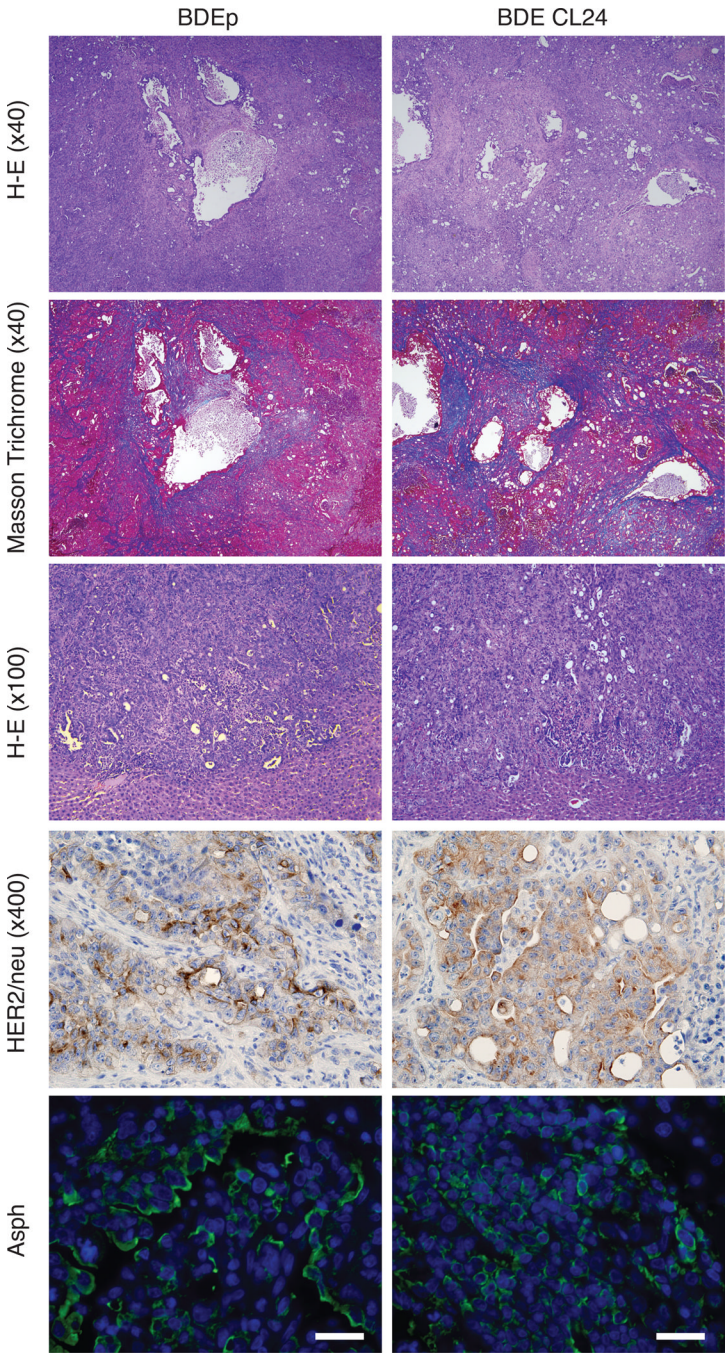

Figure 6. Histopathologic features of ICC tumors

Hematoxylin-eosin staining in central portion of tumors (upper panel 40x, and middle panel 100x), Masson Trichrome staining (upper middle panel 40x), HER2/neu and ASPH expression by immunohistochemical staining in rat liver tumors after bile duct ligation and BDEneu-p or BDEneu-CL24 inoculation into the liver parenchyma and harvested 18 days later (lower middle panel 400x magnification). ICC tumors were also immunostained with an anti-ASPH antibody (green) and DAPI (blue) (lower panel; bar, 50 μm) and demonstrated intense cell surface expression.

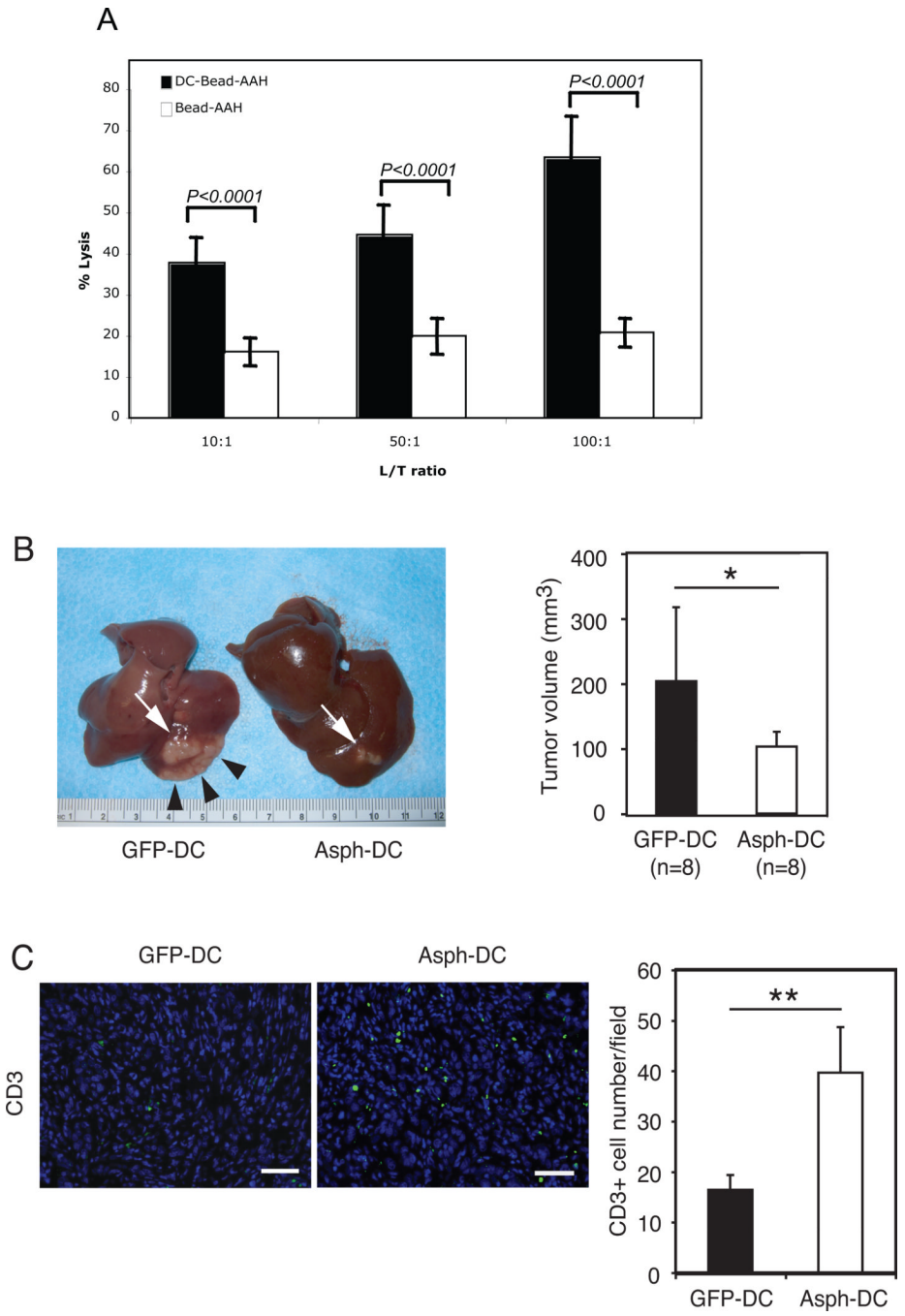

Figure 7. Immunotherapy with ASPH-loaded DCs induced anti-tumor effects with accumulation of tumor-infiltrating lymphocytes

A. Cytotoxicity against rat BDEneu-CL24 cholangiocarcinoma cells exhibited by splenocytes isolated from rats immunized with ASPH-loaded DCs compared to ASPH-coupled microbeads alone. Note the striking cell killing at various L/T ratios (**B**) Representative comparison of the morphology of ICC after GFP- or ASPH-loaded DC immunization (there were 8 animals in each group). Rats inoculated with GFP-loaded DCs showed robust growth of main tumor (white arrow) with intrahepatic spreads (arrow heads). In contrast, immunization with ASPH-loaded DCs substantially suppressed tumor growth. Comparison of tumor volumes 18 days after BDEneu-C24 inoculation into the liver were

also obtained (right panel). (**C**) Infiltration of CD3+ T lymphocytes into the ICC tumor of rats immunized with either GFP- or ASPH-loaded DCs (bar, 50 μm). In addition, the mean number of CD3+ cells in ICC tumors sections derived from animals treated with GFP- or ASPH-loaded DCs, respectively, was determined (right panel). Results represent the mean CD3+ cell number per five microscopic fields randomly selected from each tumor section. The values in all panels represents the mean ± SD. *, $p<0.05$; **, $p<0.01$.